Spatial Zonation of Landslide Prone Area Using Information Value in the Geologically Fragile Region of Samdrup Jongkhar-Tashigang National Highway in Bhutan

Thongley Thongley and Chaiwiwat Vansarochana*

Faculty of Agriculture, Natural Resource and Environment, Naresuan University, Thailand

ARTICLE INFO

Received: 15 Jul 2020
Received in revised: 28 Oct 2020
Accepted: 16 Nov 2020
Published online: 9 Dec 2020
DOI: 10.32526/ennrj/19/2020171

Keywords:
Information value/ Kappa index/ Area under the curve

*** Corresponding author:**
E-mail: chaiwiwatv@gmail.com

ABSTRACT

Samdrup Jongkhar-Tashigang National Highway (SJ-TG NH) in Bhutan experiences several landslides every year. However, there are no studies on the landslides which will assist in highway realignment. This study developed the landslide susceptibility mapping (LSM) using the information value (IV) and check the reliability of the IV. The workflow consists of landslide inventory, factor preparation, LSM development, and its validation. During the landslide inventory, a total of 130 landslides were identified from satellite image interpretation, google earth image, and field investigation. The landslide inventory was divided into a training dataset (70%) and a validation dataset (30%). Then, nine factors were used to construct a spatial database. The accuracy was conducted using the area under curve (AUC) and the reliability of the model was performed using the kappa index. The AUC for the success rate (0.7700) falls under a good category and the prediction rate (0.6798) falls under the moderate category. The kappa index (0.3407) for the IV falls under the fair reliability category. The LSM was classified into very safe (16.42%), safe (30.64%), moderately (27.67%), risky (16.18%), and high risky zones (9.09%) based on the natural break. The LSM will guide decision-makers in the realignment of the road.

1. INTRODUCTION

A landslide is the downward movement of the materials from the surface of the earth which are caused by several natural phenomena as well as induced by anthropogenic activities (Kahlon et al., 2014). The Himalayan region is considered as the youngest mountains and geo-dynamically active causing instability in the region (Chauhan et al., 2010). The number of landslides in the region is increasing every year due to deforestation, intense developmental activities, and unplanned human settlement (Chauhan et al., 2010). The landslides cause serious concern due to the loss of life, damage to the infrastructure, natural resources, etc. and pose a serious problem for future developmental activities (Kanungo et al., 2008). According to a global risk analysis report published by the world bank, landslides stood as the seventh most dangerous natural disaster and it claimed the lives of 18,200 people between 1980 to 2000 (Dilley et al., 2005). The study of landslide risk and hazard has become one of the major topics for geoscientists and engineers in recent years due to increasing awareness of its socio-economic impacts and the urbanization in mountainous areas (Aleotti and Chowdhury, 1999).

There are several methods to assess landslides which are broadly categorized into a qualitative approach and a quantitative approach. Both approaches works on the principle of past and present to the future which means the past and present landslide events will help in predicting the future landslides. The qualitative approach such as Analytical Hierarchy Process and Weighted Linear Combination works entirely based on the knowledge of the experts (Aleotti and Chowdhury, 1999). The quantitative approach is data-driven, and it is classified into a deterministic and statistical approach. The deterministic approach is appropriate for the smaller area due to its requirement for an exhaustive geotechnical test (Aleotti and

Citation: Thongley, Vansarochana C. Spatial zonation of landslide prone area using information value in the geologically fragile region of Samdrup Jongkhar-Tashigang national highway in Bhutan. Environ. Nat. Resour. J. 2021;19(2):122-131. (https://doi.org/10.32526/ennrj/19/2020171)

Chowdhury, 1999). In recent years, the statistical approach in conjunction with GIS has become more popular for the LSM due to high predictive power, cheap, easy calculation, and ability to handle the large data (Mandal and Mandal, 2018). Among the various statistical approaches, this study uses information value (IV) for the landslide assessment.

Bhutan lies in the Himalayan region with an area of 38,394 km^2 sandwiched between China and India. Bhutan is prone to several natural disaster hazards due to its location in the fragile geological setting and active seismic zone (Keunza et al., 2004). The rugged terrain and heavy monsoon precipitation intensify the landslide risk in the country. The Samdrup Jongkhar-Tashigang National Highway (SJ-TG NH) in Bhutan experiences several landslides during the monsoon season. However, the government keeps on maintaining the same route without changing the alignment and the same problem persists every year. The development of infrastructure along the highway will further destabilize the area. The unstable area may erode natural resources such as minerals, forests, threaten wildlife, and pollute water (Geertsema et al., 2009). The landslide also threatens properties, agricultural lands, and human lives.

There is no landslide risk map to guide the decision-makers for the re-alignment of the road, even though some portion of the 180 km SJ-TG NH is located in the most landslide-prone areas. Therefore, the main objective of this study is to develop, assess, and validate the LSM along the SJ-TG NH in Bhutan using the information value (IV) model. This study also aimed at checking the reliability of the IV model using the kappa index.

2. METHODOLOGY

The overall methodology of the research is shown in Figure 1. The workflow consists of landslide inventory, influencing factor preparation, developing LSM, and its validation.

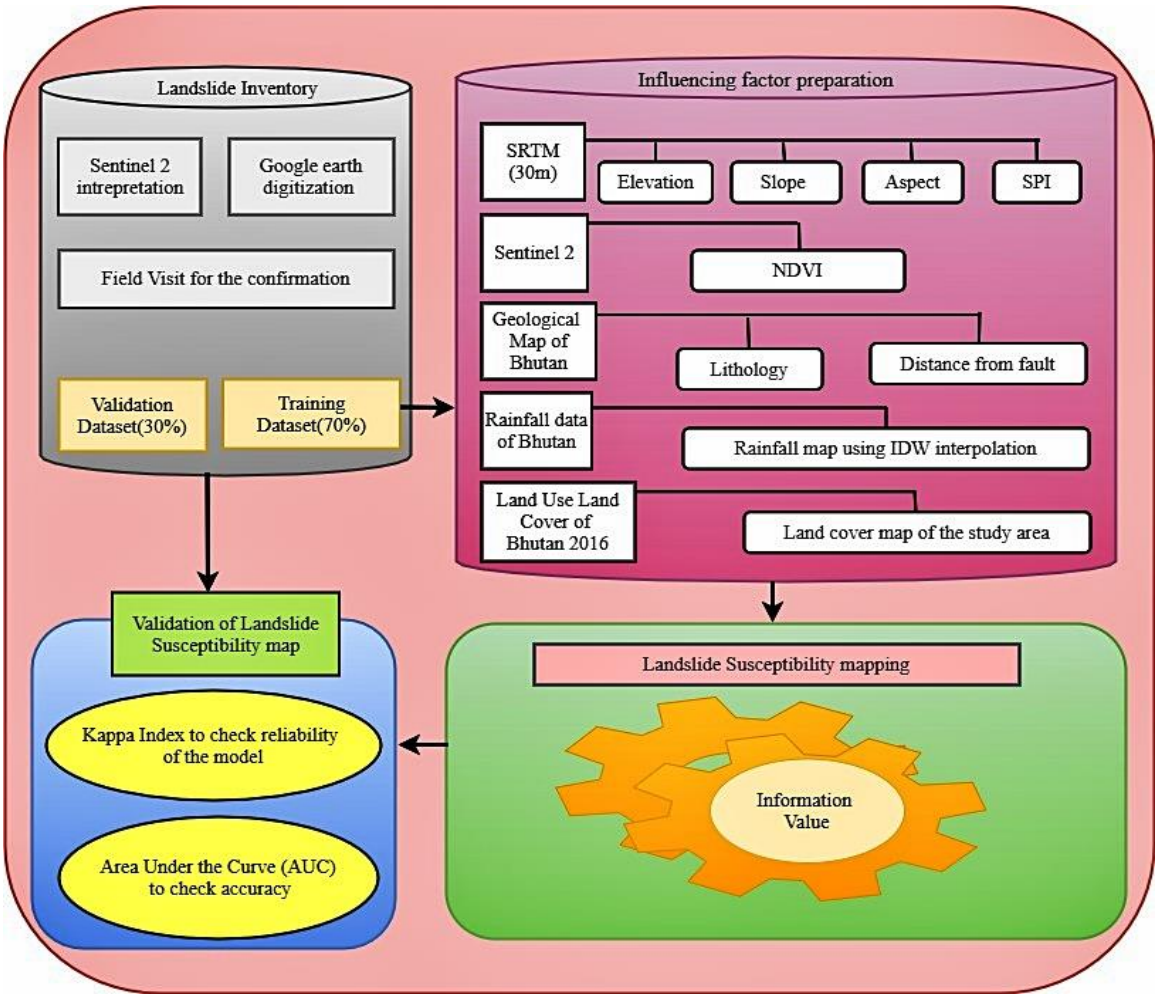

Figure 1. Flowchart of preparing the landslide susceptibility mapping

2.1 Study area

The study area (Figure 2) is located along the SJ-TG NH in Bhutan with a buffer distance of 3 km on both sides of the highway. Geographically, the study area is located between 26°48'0"N to 27°21'0"N latitude and 91°27'30"E to 91°30'0"E longitude with altitude ranging from 156 to 3,700 m.a.s.l. The highway stretches approximately 180 km connecting the Eastern districts of Bhutan. SJ-TG NH is the only highway connecting the four Eastern districts with the rest of the places of Bhutan. Moreover, the highway is the main door to the international border of Assam State of India. The area experiences several landslides every year due to its topographic nature and geological setting. The detail of lithology in the study area is given in Table 1.

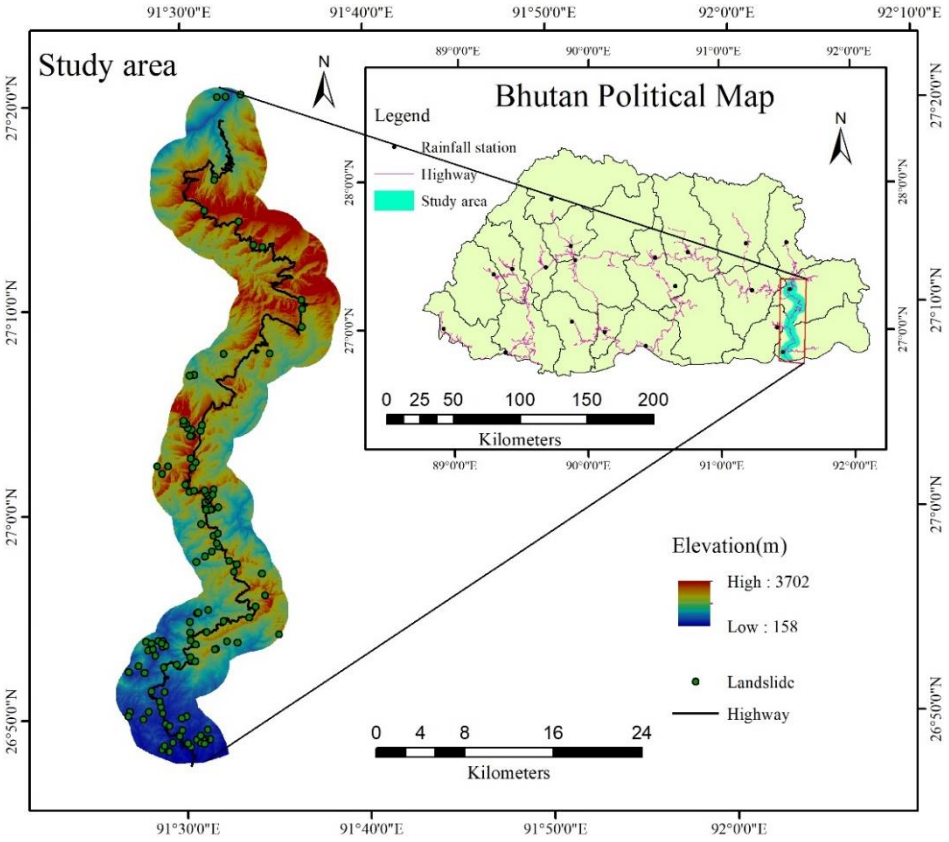

Figure 2. Study area showing the elevation, landslide locations, and rainfall stations

Table 1. Detail description of the lithology of the study area

Code	Lithological description
Tsm	Medium to coarse grained sandstone and pebble to cobble conglomeratic sandstone.
Tsl	Massive weathering siltstone and shale, interbedded with tan to gray, fine-grained, lithic-rich sandstone.
Pzg	Gray, medium grained, feldspathic, lithic-rich sandstone interbedded with dark gray to black, thin to medium-bedded, carbonaceous siltstone, shale, slate, and argillite, and rare black coal beds
Tsu	Medium to coarse grained sandstone and pebble to cobble and boulder conglomerate, interbedded siltstone.
GHlo	Massive weathering, granite-composition orthogneiss; generally, exhibits leucosomes and abundant feldspar augen. Paragneiss, schist, and quartzite intervals locally split out.
pCs	Light gray to white, tan-weathering, very fine grained, medium to thick-bedded, cliff forming quartzite. Interbeds of thin to thick bedded, green, muscovite biotite schist and phyllite with diagnostic sigmoidal quartz.
pCd	Dominated by schist and phyllite. Quartzite is thin to medium quartzite bedded, and medium gray limestone.
Pzd	Green-gray, pebble to cobble, slate-matrix diamictite
GHlml	Dominantly amphibolite-facies metasedimentary rocks, including quartzite, and biotite-muscovite-garnet schist and paragneiss often exhibiting kyanite, sillimanite, or staurolite, and partial melt textures
Tgr	Massive to foliated, syn-Himalayan leucogranite plutons
Pzj	Gray, biotite rich, locally garnet bearing schist, interbedded with biotite lamination, lithic clast-rich quartzite.

2.2 Landslide inventory mapping

The landslide inventory map shows the spatial distribution of the landslide location, types, and timing of the event of the existing landslides (Achour et al., 2017). The landslide inventory is used to find the relationship between the landslide events and its factors (Saha et al., 2005). In this study, landslide inventory was done using the google earth, satellite image interpretation, and field verification using handheld GPS. The SJ-TG NH experiences all types of landslides with the majority of translational slides and debris flow. A total of 130 landslides (Figure 2) were identified of which 91 landslides were used for the training dataset and the remaining 39 landslides were used for validation datasets.

2.3 Landslide influencing factor preparation

The landslide influencing factors used for this study were elevation, slope, aspect, stream power index (SPI), normalized difference vegetation index (NDVI), distance from the fault, lithology, rainfall map, and land cover map. The SRTM DEM (30 m) was used to derive elevation, slope, aspect, and SPI. The NDVI was prepared using sentinel 2. The geological map of Bhutan (1:500,000) prepared by Long et al. (2011) was used to extract the fault and lithological map of Bhutan. The detail of lithology is elaborated in Table 1. The average annual rainfall map was prepared using inverse distance weighting interpolation from 20 rainfall stations (Figure 2) across Bhutan from 1996 to 2017. The rainfall data was shared by the National Center of Hydrology and Meteorology. The land cover map was extracted from the Bhutan land cover map 2016 and it was prepared by the Department of Forests and Park Services. The factors were shown in Figure 3.

2.4 Information value (IV)

The information value (IV) model was developed by Yin and Yan (1988) for the prediction of slope instability. The IV creates a spatial relationship between the landslide event (landslide inventory) and its factors (Achour et al., 2017). If the IV value is positive, the landslide possibility is higher and vice versa (Chuanhua and Xueping, 2009). As per Chuanhua and Xueping (2009), IV is calculated using equation 1.

$$IV = \ln \frac{\frac{Npix(Si)}{Npix(Ni)}}{\frac{SNpix(Si)}{SNpix(Ni)}} \quad (1)$$

Where; IV is the information value of the factor's class, Npix(Si) is the number of pixels containing landslides in a factor's class, Npix(Ni) is the number of pixels in a factor's class, SNpix(Si) is the number of pixels that containing landslides in the entire study area, and SNpix(Ni) is the total number of pixels in the entire study area.

The resulting value of the IV is used for the reclassification of the factors. The reclassified factors were summed up using equation 2 to obtain the LSM.

$$LSM = F1 + F2 + \ldots. Fn \quad (2)$$

Where; F represents reclassified factors using the weight from the information value.

3. RESULTS AND DISCUSSION

3.1 Relationship between the factors and the landslide event

The result of the landslide susceptibility assessment using the IV for the individual classes of the factors is given in Table 2. The chances of the landslide are higher for the higher IV.

From Table 2, it is noticed that the IV decreases with an increase in elevation. The lowest elevation class (158-741) corresponds to the highest IV (0.738) while the highest elevation class (2480-3702) corresponds to the lowest IV (-1.351). This shows that the lower elevation of an area experiences more landslides compared to the higher elevation. This may be due to higher precipitation and fragile geology in the lower elevation. A similar trend of results was shown by Chen et al. (2014).

In contrast to elevation, the IV increases with increases in the slope angle indicating more landslide probability in the steeper slope. The IV for slope angle 0°-14.67° is -0.412 while the IV for slope angle 37.29°-46.03° is 0.657. During the site investigation, the result confirmed that the steeper slopes experienced relatively more landslides. Singh and Kumar (2018) also noticed that the steeper slope is more prone to landslides.

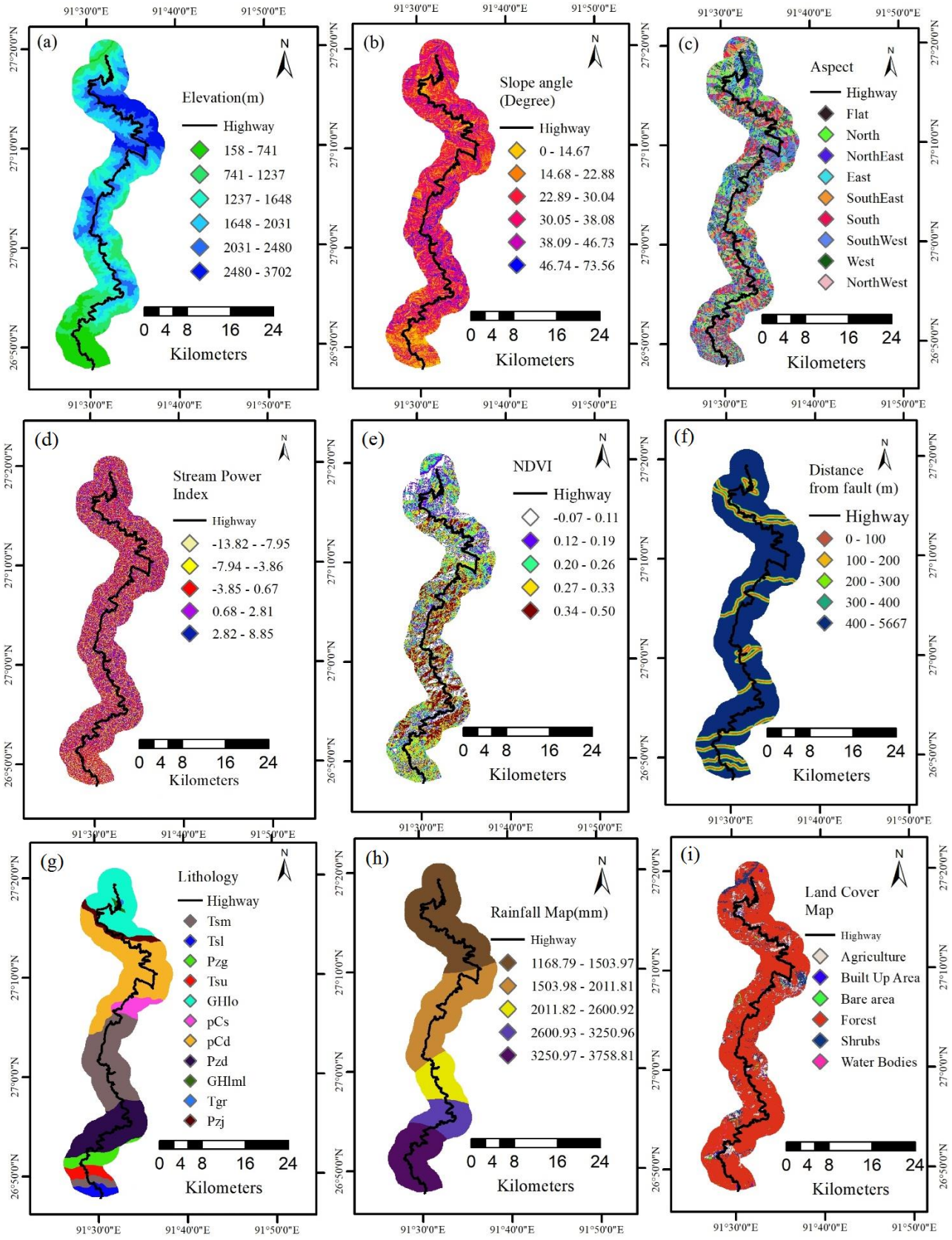

Figure 3. Factors (a) elevation, (b) slope angle, (c) aspect, (d) stream power index, (e) NDVI, (f) distance from fault, (g) lithology, (h) rainfall map, and (i) land cover map

Table 2. Relationship between the landslide event and the factors using the information value

Factor	Class	No of pixel in class	% of the pixel in class	No of landslide	% of landslide	IV
Elevation (m)	158-741	72131	12.079	23	25.275	0.738
	741-1,237	87104	14.586	15	16.484	0.122
	1,237-1,648	126532	21.189	16	17.582	-0.187
	1,648-2,031	146385	24.513	21	23.077	-0.06
	2,031-2,480	114326	19.145	14	15.385	-0.219
	2,480-3,702	50687	8.488	2	2.198	-1.351
Slope (degree)	0-14.67	59424	9.951	6	6.593	-0.412
	14.68-22.88	114980	19.254	13	14.286	-0.298
	22.89-30.04	144336	24.170	15	16.484	-0.383
	30.05-37.28	139679	23.390	18	19.780	-0.168
	37.29-46.03	98687	16.526	29	31.868	0.657
	46.04-73.56	40059	6.708	10	10.989	0.494
Aspect	Flat	7	0.001	0	0.000	0.000
	North	83659	14.009	4	4.396	-1.159
	Northeast	58950	9.872	7	7.692	-0.249
	East	56862	9.522	9	9.890	0.038
	Southeast	70077	11.735	20	21.978	0.627
	South	83741	14.023	30	32.967	0.855
	Southwest	90412	15.140	11	12.088	-0.225
	West	75084	12.573	8	8.791	-0.358
	Northwest	78373	13.124	2	2.198	-1.787
SPI	-13.82 to -7.95	46929	7.859	5	5.495	-0.358
	-7.94 to -3.86	113194	18.955	18	19.780	0.043
	-3.85 to 0.67	187826	31.453	30	32.967	0.047
	0.68 to 2.81	186860	31.291	28	30.769	-0.017
	2.82 to 8.85	62356	10.442	10	10.989	0.051
NDVI	-0.07-0.11	82147	13.756	14	15.385	0.112
	0.12-0.19	127449	21.342	24	26.374	0.212
	0.20-0.26	140709	23.563	30	32.967	0.336
	0.27-0.33	140934	23.601	20	21.978	-0.071
	0.34-0.50	105926	17.738	3	3.297	-1.683
Distance from the fault (m)	0-100	32903	5.510	12	13.187	0.873
	100-200	27860	4.665	11	12.088	0.952
	200-300	29991	5.022	3	3.297	-0.421
	300-400	24410	4.088	4	4.396	0.073
	400<	482001	80.715	61	67.033	-0.186
Lithology	Tsm	143711	24.066	37	40.659	0.524
	Tsl	14975	2.508	6	6.593	0.967
	Pzg	25318	4.240	2	2.198	-0.657
	Tsu	17511	2.932	7	7.692	0.964
	GHlo	90638	15.178	5	5.495	-1.016
	pCs	22264	3.728	6	6.593	0.570
	pCd	162213	27.164	27	29.670	0.088
	Pzd	99416	16.648	1	1.099	-2.718
	GHlml	2477	0.415	0	0.000	0.000
	Tgr	675	0.113	0	0.000	0.000
	Pzj	17967	3.009	0	0.000	0.000

Table 2. Relationship between the landslide event and the factors using the information value (cont.)

Factor	Class	No of pixel in class	% of the pixel in class	No of landslide	% of landslide	IV
Rainfall (mm/year)	1,168.79-1,503.97	202545	33.918	7	7.692	-1.484
	1,503.98-2,011.81	163862	27.440	13	14.286	-0.653
	2,011.82-2,600.92	62304	10.433	26	28.571	1.007
	2,600.93-3,250.96	59427	9.952	9	9.890	-0.006
	3,250.97-3,758.81	109027	18.257	36	39.560	0.773
LULC	Agriculture	39374	6.593	1	1.099	-1.792
	Built up area	4292	0.719	4	4.396	1.811
	Bare area	4130	0.692	1	1.099	0.463
	Forest	507583	84.999	78	85.714	0.008
	Shrubs	39286	6.579	7	7.692	0.156
	Water bodies	2500	0.419	0	0.000	0.000

In the case of the slope aspect, the IV is higher for the south-facing slope and the south-east facing slope. This reveals that the south-facing slopes encounter more landslides. This may be due to the orographic effect of the giant Himalayan Mountain which blocks the air from the Indian Ocean, condense it, and finally precipitate on the south-facing slopes. Saha et al. (2005) also observed that the south-facing slopes encounter more landslides in the Himalayan Region.

Regarding the SPI, the IV does not follow the orderly trend with the SPI value. However, it is noticed that the IV is slightly higher for the higher SPI classes. The SPI shows the erosive power of the flowing water. Higher SPI indicates higher erosive power and increases the risk of landslides.

On the other hand, the IV gradually decreased with an increase in NDVI value and the result is agreed with the result of Ba et al. (2017). The higher NDVI indicates healthy vegetation and vice versa. The decrease in IV with an increase in NDVI signifies that there is less probability of landslide in the healthy vegetated area.

Similarly, the IV decreases with an increase in distance from the fault. This clearly shows the possibility of landslide decreases as we go further from the fault and a similar result was noted by Achour et al. (2017). This is due to the weak lithology along the fault and the stability increases as we go away from faults.

The detail of lithology is explained in Table 1. The order of the highest to the lowest IV for the various lithology are Tsl, Tsu, pCs, Tsm, pCd, Pzg, GHlo, and Pzd with the IV 0.967, 0.964, 0.570, 0.524, 0.088, -0.657, -1.016, and -2.718, respectively, while GHlml, Tgr, and Pzj do not influence the landslides with zero IV.

The lowest IV (-1.484) corresponds to the lowest rainfall class (1,168.79-1,503.97). Although the IV does not follow the systematic trend with rainfall intensity for this study, it is observed that the IV increases with an increase in rainfall intensity, and the result resembles the result of Ba et al. (2017). This shows rainfall is one of the triggering factors for the landslides.

Regarding land use, the relationship between the IV and land use is still debatable in many studies. In this study, the highest IV (1.811) corresponds to the built-up area, followed by bare area (0.463), shrubs (0.156), forest (0.008), and agriculture (-1.792). The built-up area disturbs the natural topography and weakens the slopes which ultimately increase the landslides risk.

3.2 Landslide susceptibility mapping

The LSM using statistical analysis works on the principle of past and present landslide events to the future landslide zonation (Aleotti and Chowdhury, 1999). The LSM was developed using the IV which is a part of statistical analysis. The final LSM (Figure 4) is generated by reclassifying the factors using the IV from Table 2 and summing up all the reclassified factors using equation 2. The final LSM needs to classify for the better visualization and zonation of the landslide risk (Jaafari et al., 2014). The natural break classification was selected for this study due to its distinct breakpoint between the groups (Toshiro, 2002). The LSM was classified into five classes which include very safe (16.42%), safe (30.64%), moderately (27.67%), risky (16.18%), and high risky zones

(9.09%). The cost of the repeated maintenance and clearing of the highway due to landslide is much higher than the initial cost of highway construction in the long run. This research will guide the decision-makers to avoid a very high-risk landslide zone during the realignment of the highway.

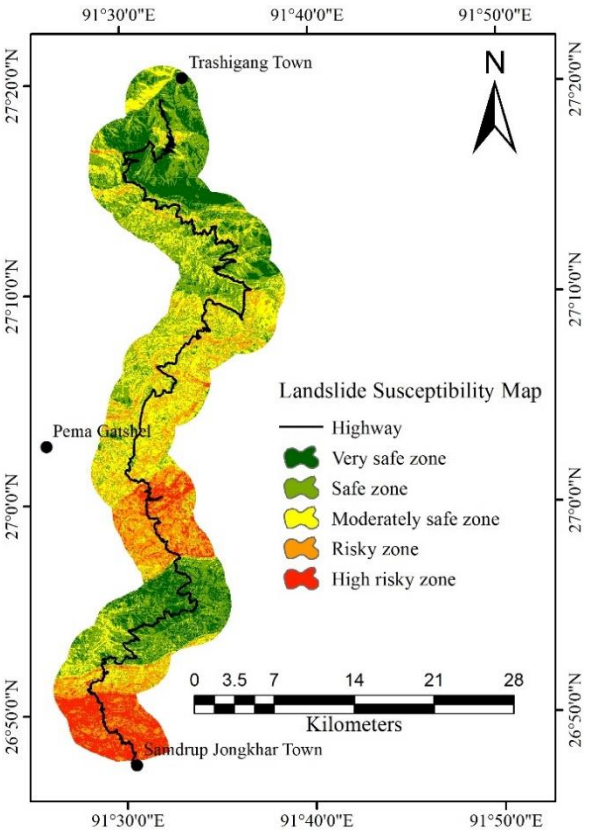

Figure 4. Landslide susceptibility map along Samdrup Jongkhar-Tashigang highway

3.3 Evaluation of the reliability of the information value for the landslide susceptibility mapping

The reliability of the model was performed by the kappa index and its value ranges from -1 (non-reliable) to 1 (reliable). As per Shirzadi et al. (2017), the kappa index is calculated based on equation 3 to equation 5.

$$\text{Kappa} = \frac{P_{obs} - P_{exp}}{1 - P_{exp}} \quad (3)$$

$$P_{obs} = \frac{TP+TN}{n} \quad (4)$$

$$P_{exp} = \frac{(TP+FN)(TP+FP)+(FP+TN)(FN+TN)}{n^2} \quad (5)$$

Where; P_{obs} (observed agreements), P_{exp} (expected agreements), and n (total pixel of the training dataset), TP (true positive), TN (true negative), FP (false positive), and FN (false negative).

As per Landis and Koch (1977), the kappa value is interpreted as shown in Table 3. For this study, the Kappa value of the IV model is 0.3407 and it falls under the fair category for the reliability of the IV model. The fair category of the model shows the fair capability of the IV model to perform LSM.

Table 3. Interpretation of the Kappa statistics scale

Kappa statistics	Strength of agreement
≤0.00	Poor
0.00-0.20	Slight
0.21-0.40	Fair
0.41-0.60	Moderate
0.61-0.80	Substantial
0.81-1.00	Almost perfect

3.4 Validation of landslide susceptibility mapping

The landslide map was validated using the area under the curve (AUC) of the receiver operating characteristic (ROC) curve. The AUC value ranges from 0.5 to 1 with AUC value 1 indicating perfect prediction (Tien Bui et al., 2019). The ROC curve was plotted using 1-specificity on the x-axis and sensitivity on the y-axis (Tien Bui et al., 2019). The sensitivity and specificity were calculated using equation 6 and equation 7

$$\text{Sensitivity} = \frac{TP}{TP+FN} \quad (6)$$

$$\text{Specificity} = \frac{TN}{TN+FP} \quad (7)$$

Where; TP (true positive), TN (true negative), FP (false positive), and FN (false negative).

The success rate curve was generated using the training dataset (70%, 91 landslides location) while the prediction rate is developed using the validation dataset (30%, 39 landslides). The success rate shows how well the resulting landslide map was classified using the existing landslides while the prediction rate indicates the predictive power of the landslide map (Jaafari et al., 2014).

From the validation result, the success rate was 0.7700 (Figure 5(a)) while the prediction rate was 0.6798 (Figure 5(b)). As per Shirani et al. (2018), the AUC is interpreted as excellent (0.9-1.0), very good (0.8-0.9), good (0.7-0.8), moderate (0.6-0.7), and poor (0.5-0.6). From the scale, the success rate (0.7700) falls under a good category while the prediction rate (0.6798) falls under the moderate category.

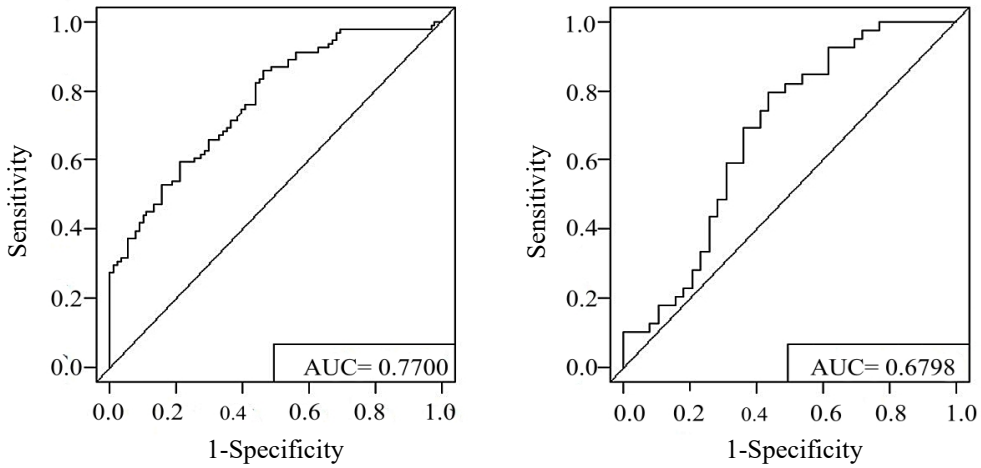

Figure 5. Validation (a) success rate curve, (b) prediction rate curve

4. CONCLUSIONS

This paper presents the LSM developed using the IV along the SJ-TG NH in Bhutan. The reliability of the LSM was checked using the Kappa index and its value of 0.3407 falls under the fair category (0.2-0.4) (Landis and Koch, 1977). Similarly, the LSM has a predictive power of 0.6798 and the prediction rate falls under a moderate category (0.6-0.7) (Shirani et al., 2018). The LSM of the SJ-TG NH is expected to help decision-makers and engineers with the realignment at the critical landslide sites. It is recommended to avoid a very high-risk landslide zone which covers 9.09% of the total area during the realignment of the highway or any other infrastructure development.

This study covers a large area with minimal accuracy using the IV model. The geotechnical study is feasible for a smaller area with higher accuracy (Lei and Jingfeng, 2006). Therefore, it is recommended to do a geotechnical test in the selected sites of the study area to further validate and confirm the reliability of the LSM.

REFERENCES

Achour Y, Boumezbeur A, Hadji R, Chouabbi A, Cavaleiro V, Bendaoud EA. Landslide susceptibility mapping using analytic hierarchy process and information value methods along a highway road section in Constantine, Algeria. Arabian Journal of Geosciences 2017;10(8):194.

Aleotti P, Chowdhury R. Landslide hazard assessment: Summary review and new perspectives. Bulletin of Engineering Geology and the Environment 1999;58(1):21-44.

Ba Q, Chen Y, Deng S, Wu Q, Yang J, Zhang J. An improved information value model based on gray clustering for landslide susceptibility mapping. ISPRS International Journal of Geo-Information 2017;6(1):18.

Chauhan S, Sharma M, Arora MK. Landslide susceptibility zonation of the Chamoli Region, Garhwal Himalayas, using logistic regression model. Landslides 2010;7(4):411-23.

Chen W, Li W, Hou E, Zhao Z, Deng N, Bai H, et al. Landslide susceptibility mapping based on GIS and information value model for the Chencang District of Baoji, China. Arabian Journal of Geosciences 2014;7(11):4499-511.

Chuanhua Z, Xueping W. Landslide susceptibility mapping: A comparison of information and weights-of-evidence methods in Three Gorges Area. Proceeding of the International Conference on Environmental Science and Information Application Technology; 2009 July 4-5; Wuhan: China; 2009.

Dilley M, Chen RS, Deichmann U, Lerner-Lam AL, Arnold M. Natural Disaster Hotspots: A Global Risk Analysis. The World Bank; 2005.

Geertsema M, Highland L, Vaugeouis L. Environmental Impact of landslides. Landslides-Disaster Risk Reduction: Springer; 2009. p. 589-607.

Jaafari A, Najafi A, Pourghasemi H, Rezaeian J, Sattarian A. GIS-based frequency ratio and index of entropy models for landslide susceptibility assessment in the Caspian forest, Northern Iran. International Journal of Environmental Science and Technology 2014;11(4):909-26.

Kahlon S, Chandel VB, Brar KK. Landslides in Himalayan Mountains: A study of Himachal Pradesh, India. International Journal of IT, Engineering and Applied Sciences Research 2014;3:28-34.

Kanungo D, Arora M, Gupta R, Sarkar S. Landslide risk assessment using concepts of danger pixels and fuzzy set theory in Darjeeling Himalayas. Landslides 2008;5(4):407-16.

Keunza K, Dorji Y, Wangda D. Landslides in Bhutan. Country Report. Thimpu. Bhutan: Department of Geology and Mines, Royal Government of Bhutan; 2004. p. 8.

Landis JR, Koch GG. The measurement of observer agreement for categorical data. Biometrics 1977:159-74.

Lei Z, Jingfeng H. GIS-based logistic regression method for landslide susceptibility mapping in regional scale. Journal of Zhejiang University-Science A 2006;7(12):2007-17.

Long S, McQuarrie N, Tobgay T, Grujic D, Hollister L. Geologic map of Bhutan. Journal of Maps 2011;7(1):184-92.

Mandal S, Mandal K. Bivariate statistical index for landslide susceptibility mapping in the Rorachu River Basin of Eastern

Sikkim Himalaya, India. Spatial Information Research 2018;26(1):59-75.

Saha AK, Gupta RP, Sarkar I, Arora MK, Csaplovics E. An approach for GIS-based statistical landslide susceptibility zonation-with a case study in the Himalayas. Landslides 2005;2(1):61-9.

Shirani K, Pasandi M, Arabameri A. Landslide susceptibility assessment by dempster-shafer and index of entropy models, Sarkhoun Basin, Southwestern Iran. Natural Hazards 2018;93(3):1379-418.

Shirzadi A, Bui DT, Pham BT, Solaimani K, Chapi K, Kavian A, et al. Shallow landslide susceptibility assessment using a novel hybrid intelligence approach. Environmental Earth Sciences 2017;76(2):60.

Singh K, Kumar V. Hazard assessment of landslide disaster using information value method and analytical hierarchy process in highly tectonic Chamba Region in bosom of Himalaya. Journal of Mountain Science 2018;15(4):808-24.

Tien Bui D, Shahabi H, Omidvar E, Shirzadi A, Geertsema M, Clague JJ, et al. Shallow landslide prediction using a novel hybrid functional machine learning algorithm. Remote Sensing 2019;11(8):931.

Toshiro O. Classification Methods for Spatial Data Representation. London, UK: Center for Advanced Spatial Analysis University College London; 2002.

Yin K, Yan, T. Statistical prediction model for slope instability of metamorphosed rock. Proceedings of the 5th International Symposium on Landslides; 1988 Jul 10; Lausanne: Switserland; 1988. p. 1269-72.